Astron. Astrophys. 341, 216–223 (1999)

ASTRONOMY
AND
ASTROPHYSICS

On the magnetic field and circumstellar environment of the young O7 star θ^1 Orionis C*

J.-F. Donati[1] **and G.A. Wade**[2]

[1] Laboratoire d'Astrophysique, Observatoire Midi-Pyrénées, F-31400 Toulouse, France (e-mail: donati@obs-mip.fr)
[2] Department of Physics and Astronomy, University of Western Ontario, London Ontario, N6A 3K7, Canada (e-mail: gwade@astro.utoronto.ca)

Received 23 July 1998 / Accepted 6 October 1998

Abstract. We present new circular spectropolarimetric observations of the young O-type star θ^1 Orionis C obtained with the MuSiCoS échelle spectropolarimeter and the 2 m Télescope Bernard Lyot, in an attempt to detect the surface magnetic field structure invoked to explain the periodic variability of θ^1 Ori C at X-ray, UV and optical wavelengths. We obtain null detections with 250 G 1σ error bars for the disc-averaged line-of-sight (i.e. longitudinal) component of the surface magnetic field vector, from which we conclude that the polar strength of the dipole field structure is lower than 1.6 to 2.0 kG (with a confidence level of 87%), depending on the exact orientation of the magnetic and rotation axes with respect to the line of sight.

We report as well the unexpected discovery of strong, time variable continuum circular polarisation in the spectrum of θ^1 Ori C, as well as depolarisation structures associated with nebular emission lines, indicating that this continuum polarisation (the nature of which is as yet unclear) is produced within the immediate circumstellar environment.

Key words: polarization – stars: circumstellar matter – stars: early-type – stars: individual: θ^1 Ori C – stars: magnetic fields

1. Introduction

θ^1 Orionis C (HD 37022) is a very young O7V star. As the hottest member of the Orion Trapezium, it represents the main source of ionising photons for the entire surrounding nebula. It exhibits strictly periodic variability, suggestive of a magnetic rotator: Hα and He II (468.6 nm) emission, ultraviolet C IV (154.8 and 155.0 nm) wind lines, photospheric absorption lines, and ROSAT X-ray emission all appear to vary, either in relative phase or antiphase, with a single well-defined period of 15.426 ± 0.002 d (Stahl et al. 1993, 1996; Walborn & Nichols 1994; Gagné et al. 1997; Stahl 1998).

This behaviour is reminiscent to that of middle-main sequence magnetic chemically peculiar stars, the Ap, Bp, He-weak and He-strong stars. These objects, which often possess strong, approximately dipolar magnetic fields, show photometric variability, line strength and shape variability, and line polarisation variability which occur with a single well-defined period: the rotational period of the star (e.g. Mathys & Manfroid 1985; Wade et al. 1997a, b). These phenomena are interpreted as *rotational modulation* caused by the stellar magnetic structure (tilted with respect to the rotation axis) and associated surface abundance inhomogeneities (thought to be generated by the interplay between diffusion, mass loss and circulation processes in their atmospheres in the presence of a magnetic field, e.g. Babel 1992). In some cases, variable, asymmetric Hα emission, variable ultraviolet C IV resonance line absorption, nonthermal radio emission and X-ray emission are also observed, probably indicative of a magnetically confined wind and trapped circumstellar plasma (Shore & Brown 1990; Babel & Montmerle 1997a). The striking similarity between many (although it should be noted, not all) of the phenomena displayed by these objects and those displayed by θ^1 Ori C suggests that this star may itself be a magnetic rotator and represent the O-type analogue to the magnetic chemically peculiar A and B type stars (Walborn & Nichols 1994, Stahl et al. 1996, Gagné et al. 1997).

Following this reasoning, Babel & Montmerle (1997b) applied to θ^1 Ori C their new Magnetically-Confined Wind Shock (MCWS) model originally developed to explain the X-ray emission of some Ap/Bp stars (Babel & Montmerle 1997a). In this model, a dipolar magnetic field confines and directs the stellar wind components in the two magnetic hemispheres toward the (magnetic) equatorial plane, where their collision produces a strong shock. The resulting circumstellar structure consists of a high-density, corotating equatorial "cooling disc", and a high-temperature, low-density shock and extended postshock region (Babel & Montmerle 1997a). The X-ray emission computed from the model is largely dependent on the assumed magnetic field, and provides a strong constraint on the surface magnetic field intensity. In the case of θ^1 Ori C, the MCWS model implies (from the observed X-ray emission) that the magnetic field should have a polar strength of the order of 300 G.

In this paper, we present new spectropolarimetric observations we have recently obtained for θ^1 Ori C. In Sect. 2 we briefly describe the instrument we used (the MuSiCoS spectropolarimeter) as well as the observing procedure, and provide a summary of the observations we recorded. In Sect. 3 we detail

Send offprint requests to: J.-F. Donati

* Based on data collected with the MuSiCoS spectropolarimeter of the Télescope Bernard Lyot, Observatoire du Pic du Midi, France

the new constraints on the photospheric magnetic field provided by measurements of the Zeeman effect in our spectra. In Sect. 4 we report the discovery of strong, variable continuum circular polarisation in the spectrum of this star, as well as depolarisation structures associated with all nebular emission lines. Finally, we discuss in Sect. 5 the impact of these new observations on models of θ^1 Ori C and its circumstellar environment, and we suggest further specific investigations which should help clarify our understanding of this object.

2. Observations

2.1. MuSiCoS spectropolarimetric observations

Six circularly polarised (Stokes V) and unpolarised (Stokes I) observations of θ^1 Ori C were obtained using the MuSiCoS spectropolarimeter mounted on the 2 m Téléscope Bernard Lyot (TBL) at the Observatoire du Pic du Midi, in February 1997 (four spectra) and 1998 (two spectra).

The MuSiCoS spectropolarimeter consists of an échelle spectrograph (Baudrand & Böhm 1992) and dedicated polarimetric unit (Donati et al. 1998) developed within the framework of the MuSiCoS (MUlti-SIte COntinuous Spectroscopy) international collaboration (Catala et al. 1993). The spectrograph itself is a table-top instrument, fed with a double optical fibre from the Cassegrain-mounted polarimeter (inspired by the prototype of Semel et al. 1993). This instrument allows one to obtain, in a single exposure, a stellar spectrum in a given polarisation state (Stokes V in our particular case) with full wavelength coverage from 450 to 660 nm and at a resolving power of about 35,000. In normal operation, starlight entering the polarimeter at the Cassegrain focus is retarded by the rotatable quarter-wave plate. The beam then intersects a Savart-type beamsplitter, which separates the stellar light into two beams which are respectively polarised along and perpendicular to the instrumental reference azimuth. The two beams are then focal reduced to an aperture of f/2.5 for injection into a 50/60 μm core/cladding diameter double optical fibre, which transports the light down to the spectrograph. Spectra in both orthogonal polarisation states are thus recorded simultaneously onto a 1024$\times$1024 pxl SITE CCD detector.

A complete Stokes V exposure usually consists of a sequence of four individual subexposures between which the quarter-wave plate is switched by 90° back and forth, with the result of exchanging the two beams throughout the whole instrument. With such an observing procedure, one can suppress all systematic spurious circular polarisation signals down to a relative level of at least 0.002% rms (Donati et al. 1997, 1998). Data reduction and polarisation extraction was achieved using the dedicated ESpRIT reduction package, described by Donati et al. (1997). A detailed log of the observations is given in Table 1.

Table 1. MuSiCoS spectropolarimetric observations of θ^1 Ori C. For each observation, the successive columns respectively list the UT and Julian dates, the exposure time $t_{\rm exp}$, the rotational phase ϕ (using the ephemeris ephemeris JD $= 2448833.0 + 15.426E$ of Stahl 1998), the peak S/N per 4.5 km s^{-1} pxl in the raw spectrum, and the relative rms noise level $N_{\rm LSD}$ (per 4.5 km s^{-1} velocity bin) in the resulting "Least-Squares Deconvolved" Stokes V spectra (see Sect. 3).

Date	JD 2,450,000+	$t_{\rm exp}$ min	ϕ	S/N pxl^{-1}	$N_{\rm LSD}$ %
1997 Feb. 20	500.3453	40	0.087	280	0.14
1997 Feb. 22	502.3429	40	0.216	450	0.08
1997 Feb. 23	503.3230	40	0.280	140	0.30
1997 Feb. 25	505.3160	40	0.409	300	0.14
1998 Feb. 15	860.4021	40	0.428	250	0.13
1998 Feb. 26	871.3354	20	0.136	270	0.13

3. An upper limit for the magnetic field

We have attempted to detect the characteristic Zeeman variation of circular polarisation across absorption lines caused by the presence of a magnetic field in the line-forming region. We follow Donati et al. (1997) and employ the new cross-correlation technique called "Least-Squares Deconvolution" (LSD) developed specifically for spectropolarimetric observations. The idea underlying this technique is to extract a mean Stokes V profile from many individual spectral lines simultaneously in order to improve the signal to noise ratio S/N.

3.1. Least-squares deconvolution of spectral lines

The selection of spectral lines to be used for LSD must be done carefully. As detailed by Stahl et al. (1996), optical emission lines (for example Hα or the He II 468.6 nm line) show a rotational modulation opposite to that of photospheric lines, implying that both sets of lines probe totally different plasmas and therefore probably very different magnetic field strengths and orientations as well. For the particular purpose of LSD, we selected only photospheric lines, as we wish to estimate the magnetic field at the stellar surface. Note that some of the remaining He lines (the He II feature at 454.1 nm for instance) were also discarded, even though they probably form in the photosphere (Stahl et al. 1996); the strong intrinsic broadening to which they are subject would blur out any potential Zeeman signature from the magnetic field.

Altogether, only about 15 different spectral lines (due to He, C, N and O) could been used for LSD throughout the available domain, yielding an average multiplex gain in S/N (defined as the ratio between the S/N in the final LSD spectrum to the peak S/N in the raw spectrum, see Table 1) of the order of 2.7. Note that the spectra recorded on 1997 Feb. 25 and 1998 Feb. 15 correspond to almost identical rotational phases (0.419 within about 1%); the associated LSD Stokes V profiles were therefore averaged together to decrease the relative noise level down to 0.09% rms (per 4.5 km s^{-1} velocity bin).

A single LSD Stokes I and V profile of θ^1 Ori C is shown in Fig. 1. The mean Stokes I profile we obtain is quite compatible with the 50 km s^{-1} total (i.e. rotational plus turbulent) broadening reported by Stahl et al. (1996), and gives confidence that we

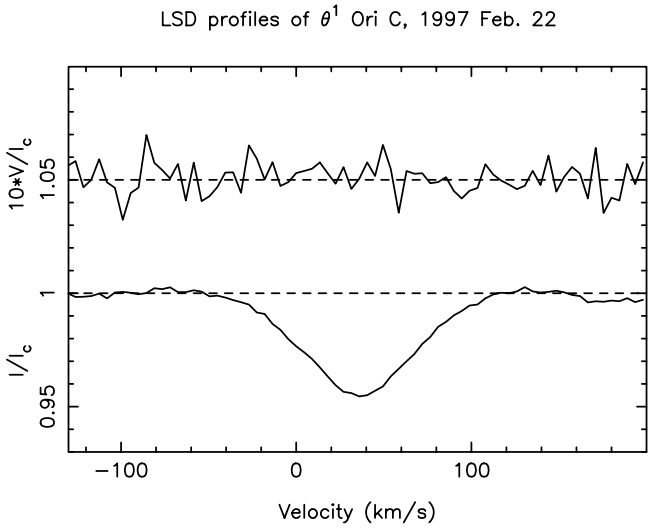

Fig. 1. LSD Stokes V (upper curve) and I (lower curve) profiles of θ^1 Ori C on 1997 Feb. 22. Note that the Stokes V profile was expanded by a factor of 10 and shifted upwards by 1.05 for graphics purposes.

have succeeded in excluding most lines with non-photospheric contributions from the analysis. Note as well that the radial velocity of θ^1 Ori C is now 36 ± 2 km s^{-1} and not 10 km s^{-1} as reported by Stahl et al. (1996), thus confirming the new measurements of Stahl (1998). Clearly, this star undergoes long term radial velocity changes, the origin of which is still unclear.

3.2. Assumed field geometry

Although we have no Stokes V Zeeman detection to report, our observations can be useful to derive upper limits on the strength of any dipolar magnetic field which may be present at the stellar surface. Two methods are available for this purpose. The first one consists in deriving a disc-averaged estimate (and error bar) of the line-of-sight projected (i.e. longitudinal) component of the stellar magnetic field vector from the first moment of the LSD Stokes V profiles (e.g. Mathys 1991; Donati et al. 1997). The second one involves computing the Zeeman signatures for a given magnetic structure and seeing how strong the polar field can be before the corresponding synthetic Stokes V signatures are detectable, given the noise level in our spectra.

The results of both techniques obviously depend on the assumed structure of the large scale magnetic field, as well as its geometry with respect to the observer. We assume here (following Babel & Montmerle 1997b) that the field is a centred dipole whose magnetic axis is tilted at an angle β with respect to the rotation axis of the star. We denote by i the angle between the rotation axis and the line of sight, and by ϕ_0 the rotational phase at which the angle between the magnetic axis and the line of sight is minimum. From the observation that high velocity absorption in UV stellar wind lines (presumably due to fast wind streams from the magnetic pole intersecting the line of sight) is strongest at rotational phase 0.5 (Stahl et al. 1996), we can infer that $\phi_0 = 0.5$ and $i - \beta$ (the angle between the magnetic axis and the line of sight at phase 0.5) is not large (Stahl et al. 1996 propose $i \simeq \beta$ but quote no quantitative upper limit on $|i - \beta|$). In addition to this and according to the MCWS model of Babel & Montmerle (1997b), the X-ray light curve indicates that the magnetic equatorial plane (hosting the circumstellar cooling disc) is seen almost edge on at rotational phase 0.0, and more specifically that $85^\circ \leq i + \beta \leq 90^\circ$ (and not $0^\circ \leq i - \beta \leq 5^\circ$ as erroneously written in Babel & Montmerle 1997b).

Altogether, we obtain that the most probable magnetic geometry is that with $i = \beta = 45^\circ$, but values of i ranging from 25° (with $\beta = 65^\circ$) to 65° (with $\beta = 25^\circ$) are still possible. Values of i smaller than 25° are unlikely as they would imply line-of-sight projected rotational velocities $v \sin i$ smaller than 10 km s^{-1} (assuming a radius of 8 $R_\odot$, Howarth & Prinja 1989, and a rotation period of 15.426 d), incompatible with the short term radial velocity variations observed in photospheric line profiles of θ^1 Ori C and presumably attributable to rotational modulation (Stahl et al. 1996). Similarly, values of i larger than 65° (for which the magnetic axis would never come closer than 40° to the line of sight) are also less likely as they would imply too small a variability in the absorption of UV stellar wind lines at velocities towards the observer in excess of 2000 km s^{-1} (this point would however require confirmation through a detailed modeling of the wind structure).

3.3. Derivation from the longitudinal magnetic field

It is well known that the first moment of a Stokes V profile provides a direct way of estimating the longitudinal component of the vector magnetic field averaged over the visible hemisphere (e.g. Mathys 1991). This method can also be used directly on LSD Stokes V profiles, as demonstrated recently by Donati et al. (1997). When applied to our spectra, only non detections are obtained, with formal 1σ error bars of 370 G, 330 G, 250 G, 760 G and 260 G at rotational phases of 0.087, 0.136, 0.216, 0.280 and 0.419 respectively.

For the magnetic field geometry of θ^1 Ori C (see Sect. 3.2), it is clear that the strongest constraint on the dipole polar field strength $B_{\rm p}$ comes from our observation closest to phase 0.5 (when the angle between the magnetic axis and the line of sight is smallest), i.e. that obtained at phase 0.419. Quantitatively, disc-averaged longitudinal field B_ℓ at rotational phase ϕ is given by:

$$B_\ell \;=\; B_{\rm p}\,\frac{15+u}{20(3-u)} \times \left(\cos\beta\cos i + \sin\beta\sin i\cos 2\pi(\phi-\phi_0)\right)\;,$$

where u denotes the limb darkening parameter (Preston 1967). Given the atmospheric parameters of θ^1 Ori C (and in particular its effective temperature of 45,500 K and logarithmic surface gravity of 4.2, Howarth & Prinja 1989), we infer a limb darkening constant u at 500 nm of about 0.16 (Wade & Rucinski 1985). For $i = \beta = 45^\circ$, we obtain that polar field strengths in excess of 1.6 kG (resp. 2.7 kG) imply unsigned longitudinal fields larger than 1.5 times (resp. 2.6 times) our formal 1σ error bar of 260 G at phase 0.419, which would be detectable with a false alarm probability smaller than 13% (resp. 1%).

With this first method, we thus conclude that for $i = \beta = 45^\circ$, $B_{\rm p}$ is smaller than 1.6 kG with a confidence level of 87%, and less than 2.7 kG with a confidence level of 99%. If the angle between the magnetic axis and the line of sight at rotational phase 0.5 (i.e. $i - \beta \simeq 2i - 90$, see Sect. 3.2) is non zero, this upper limit is found to be, at first order, inversely proportional to $\sin\ 2i$, reaching values of about 2 kG (for a confidence level of 87%) when i gets as small as 25° or as large as 65° (see Sect. 3.2).

3.4. Derivation from spectrum synthesis

The second method consists in synthesising Stokes V profiles for various magnetic field strengths in order to determine the polar strength at which such Zeeman signatures are detectable (with a confidence level of, say, 87%) given a noise pattern similar to that of our observations.

For this purpose, we need to have a rough model for the average spectral line. From the radius estimate (8 $R_\odot$) obtained by Howarth & Prinja (1989) as well as the rotation period (15.426 d), we derive a line-of-sight projected rotational velocity $v \sin i$ of about 11 to 24 km s^{-1} (for values of i ranging from 25 to 65°, see Sect. 3.2). In addition to rotation, an additional intrinsic line broadening (of yet unknown origin, Stahl et al. 1996, but nevertheless fairly common in O and B stars, Howarth et al. 1997) with a Doppler width of as much as 40 km s^{-1} must be invoked to account for the total width of observed photospheric profiles (of the order of 50 km s^{-1}, see Fig. 1). The very simple spectral line model we use here involves an intrinsic profile with constant Gaussian shape over the stellar disc, a Doppler width of 40 km s^{-1} (i.e. a full width at half maximum of 67 km s^{-1}) and a relative central depth of 5%. The continuum center-to-limb darkening parameter is set to 0.16 (see Sect. 3.3). We find that the disc integrated profile we obtain with this simplistic model reproduces satisfactorily the shape of the observed Stokes I profile of θ^1 Ori C.

The model Stokes V signature we obtain for the field geometry described in Sect. 3.2 is null at phase 0.0 (when the magnetic equator, seen edge-on, is perpendicular to the projection of the rotation axis onto the plane of the sky) and largest at phase 0.5 (when the angle between the magnetic axis and the line of sight is minimum). In the particular case of a dipole magnetic field with $i = \beta = 45^\circ$ and $B_{\rm p} = 1$ kG, the relative peak-to-peak amplitude of the Stokes V signature at phase 0.5 is 0.051%. The strongest constraint we can obtain on $B_{\rm p}$ comes once more from our observation at phase 0.419. For this particular rotational phase and any given magnetic geometry, we can compute, for various polar field strengths, the corresponding *increase* in the reduced χ^2 of the Stokes V profile due to the Zeeman signature itself (with respect to a situation with pure noise, i.e. unit reduced χ^2), as well as the associated detection probability.

We first observe that this detection probability depends on the size and number of individual velocity bins throughout the line profile; while increasing the bin size reduces the relative noise level per bin and helps detecting a potential Zeeman signature, increasing it too much smears out the magnetic signal and makes its detection harder. We find that the upper limit on $B_{\rm p}$ above which the associated Zeeman signature is detected is *minimised* for an optimal velocity bin size of 18 km s^{-1} (i.e. 4 pxl). In this case, a magnetic dipole with $i = \beta = 45^\circ$ is detected with a false alarm probability of 13% (resp. 1%) if the polar field $B_{\rm p}$ is larger than 2 kG (resp. 3.4 kG). The corresponding Zeeman signature has a peak-to-peak amplitude of 0.10% (resp. 0.17%) and generates an increase in the reduced χ^2 of the Stokes V profile of the order of 50% (resp. 140%) when using about nine 18 km s^{-1} bins throughout the line profile.

With this second method, we therefore conclude that for $i = \beta = 45^\circ$, $B_{\rm p}$ is lower than 2 kG with a confidence level of about 87%, and less than 3.4 kG with a confidence level of 99%. As with the previous method (see Sect. 3.3), we find that if the angle between the magnetic axis and the line of sight at rotational phase 0.5 is non zero, the upper limit on $B_{\rm p}$ is, at first order, inversely proportional to $\sin\ 2i$, reaching values of about 2.6 kG (for a confidence level of 87%) when i gets as small as 25° or as large as 65° (see Sect. 3.2).

4. Discovery of continuum circular polarisation and depolarisation structures

We report the detection of strong continuum circular polarisation in a few of our Stokes V spectra of θ^1 Ori C. Note that technical tests carried out previously demonstrate that the fiber-fed MuSiCoS spectropolarimeter, although not as good as conventional photopolarimeters at measuring *continuum* circular polarisation, can nevertheless yield estimates at an accuracy level of about 0.8% rms (Donati et al. 1998). On 1997 Feb. 20, 22 and 25, we find that the continuum circular polarisation of θ^1 Ori C reaches relative levels of about 3.8% (see Fig. 2), 1.2% and 2.0% respectively, i.e. 4.8, 1.5 and 2.5 times larger than the average error bar quoted above. On all other nights (1997 Feb. 23 included), the measured continuum circular polarisation is of the order of a few times 0.1%, i.e. smaller than the measurement uncertainty. As well, circular and linear polarisation spectra of magnetic Ap stars and nonmagnetic standard stars (Wade et al. 1998a, b) obtained on these same nights show no similar high continuum polarisation levels, nor do they exhibit any spurious spectral features which would indicate a malfunction of the instrument. The false alarm probabilities associated with these three measurements are respectively 0.0002%, 13% and 1.2%, implying that the first one at least can be considered as a definite detection. As crosstalk from linear to circular polarisation is very small for the MuSiCoS spectropolarimeter (of the order of 0.2%, Donati et al. 1998), we can safely claim that the observed continuum polarisation is indeed mostly *circular* polarisation. We detect no variation of this continuum circular polarisation with wavelength down to the accuracy of what our instrument can reliably measure, about 0.5% rms between both spectral domain edges (Donati et al. 1998).

Clear *depolarisation structures*[1] are also observed in our V/I spectra, in conjunction with the nebular emission lines of [O III] (at 495.89 nm and 500.68 nm), [N II] (at 654.81 nm and 658.36 nm), Hα (see Fig. 2) and perhaps even Hβ. The detection of such depolarisation structures provides an independent confirmation of the reality (and astrophysical origin) of the continuum circular polarisation we measured. The relative depths of the depolarisation structure in Hα on 1997 Feb. 20, 22 and 25 are respectively equal to 2.30%, 0.55% and 1.10% with an uncertainty smaller than 0.2%, implying that the detection of line depolarisation (and therefore by inference continuum polarisation) is confirmed on all three epochs (with false alarm probabilities smaller than 0.6%). Moreover, we can conclude that the day-to-day variability we observe (possibly due to rotational modulation) is also real.

We observe that the depolarisation structures in our V/I spectra deepen with increasing line-to-continuum flux ratio, and are compatible with a constant *absolute level* of continuum circular polarisation throughout each nebular line. This strongly suggests that most nebular line flux (within the 2″ circular aperture of our instrument) is not polarised and is emitted outside the region in which the continuum polarisation is generated, implying that the production of continuum polarisation is confined to the immediate circumstellar environment. It is, however, important to note that it is only the narrow core (i.e. the nebular component) of the Hα emission that appears to be depolarised, the majority of the Hα emission being polarised to the same extent as the continuum (see Fig. 2). This implies in particular that the (presumably circumstellar) material responsible for this broad Hα emission is located inside the polarising environment.

Worth noting is the fact that no continuum polarisation (nor depolarisation structures) are detected in either Stokes V spectra recorded in 1998, although both correspond to rotational phases (0.136 and 0.428) very close to those at which continuum polarisation was strongest one year before (0.087 and 0.409). This indicates that the circular polarisation we detected is also intrinsically variable on a long term basis (in addition to the short term variability reported above and potentially attributable to rotational modulation), and is probably associated with a transient event whose possible nature is discussed in Sect. 5.

We also observe in all our spectra that both [O III] nebular lines show a strongly asymmetric profile, as illustrated for the 500.684 nm line in the particular case of our 1997 Feb. 20 observation. We find that the shape of both profiles can always be well described as the sum of two Gaussian components, a main one centred at 25 ± 1 km s^{-1} (i.e. very close to the average radial velocity of the Orion nebula, e.g. Stahl 1998) along with a weaker blueshifted one at a radial velocity of 10 ± 1 km s^{-1}. Such asymmetric profiles of the 500.684 nm [O III] nebular line in the centre of the Orion nebula were already reported and studied in detail (through multiple Gaussian fitting techniques) by Castañeda (1988); note in particular that the radial velocities of the two most intense components identified by Castañeda in the direction of θ^1 Ori C (at 23.5 and 10.8 km s^{-1} respectively) are in good agreement with our estimates. The additional depolarisation we observe in conjunction with the blueshifted component (see Fig. 3) indicates that most of the flux associated with it is unpolarised as well (just as that associated with the main component). This second component must therefore also be emitted outside the immediate polarising circumstellar environment, probably where the various flows observed in the centre of the nebula interact together, as originally proposed by Castañeda (1988). Note that all other nebular lines in the spectrum (Hα, [N II]) do not show such asymmetric profiles.

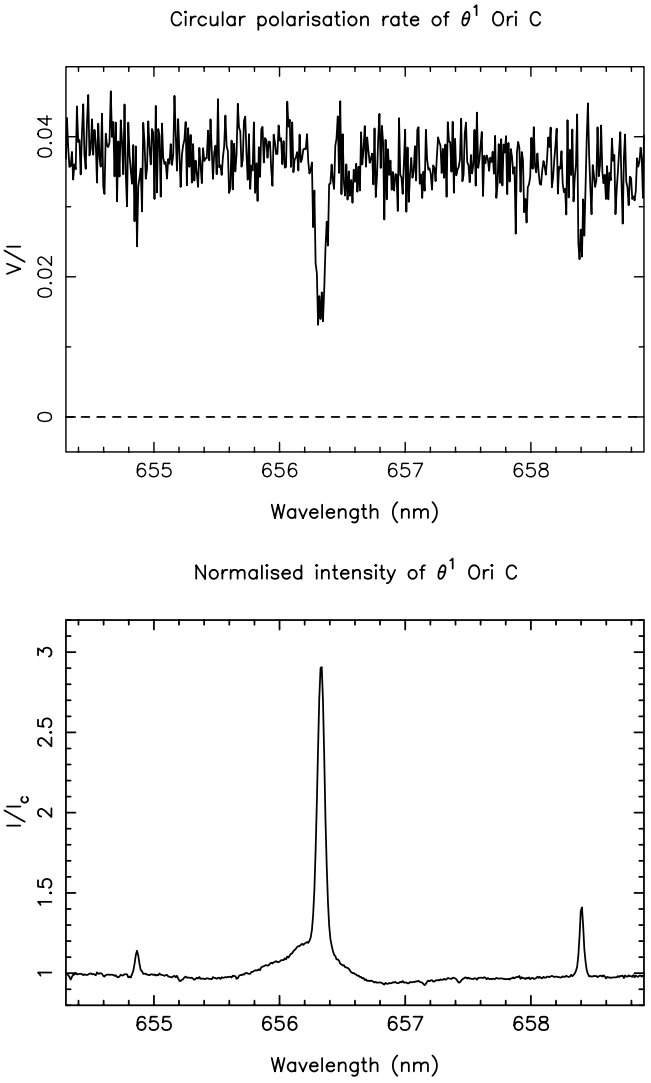

Fig. 2. Circular polarisation rate (*top panel*) and normalised intensity (*bottom panel*) of θ^1 Ori C (and background nebula) at Hα wavelengths, on 1997 Feb. 20

5. Summary and discussion

Six Stokes V spectra of θ^1 Ori C were obtained with the MuSiCoS spectropolarimeter mounted on the 2 m Télescope Bernard

[1] We emphasise that the expression 'depolarisation structure' used throughout this paper only refers to a local *decrease* in the observed polarisation rate V/I, and not to some atomic physics process (like the Hanlé effect) affecting the radiative transfer in the line forming region.

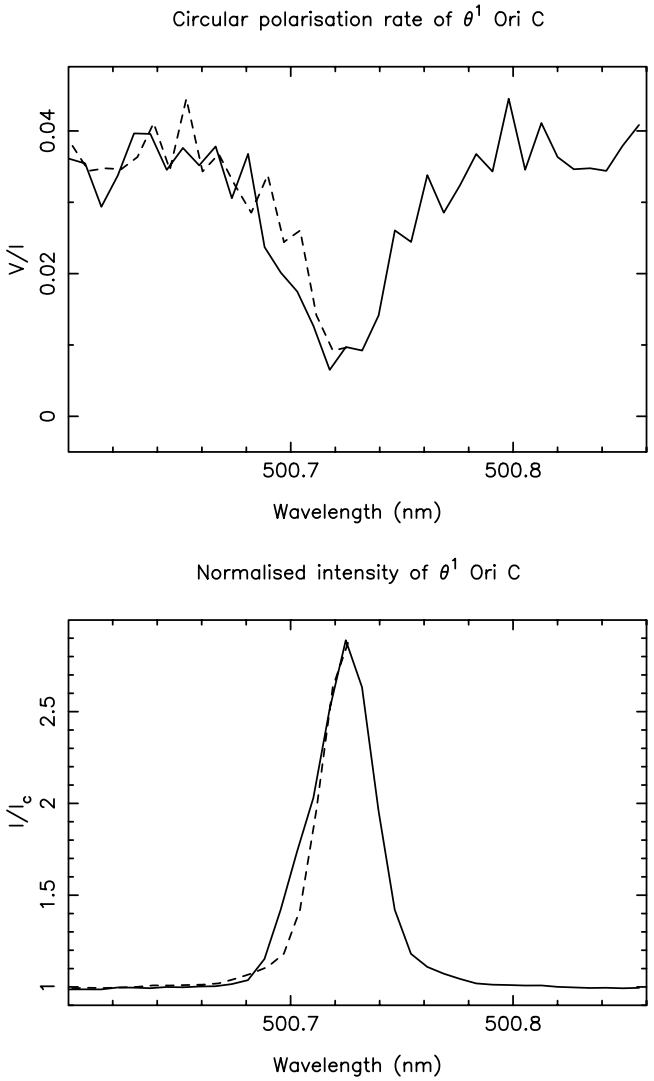

Fig. 3. Circular polarisation rate (*top panel*) and normalised intensity (*bottom panel*) of θ^1 Ori C (and background nebula) at 500.7 nm, on 1997 Feb. 20. The full lines depict the observed Stokes V and I profiles of the [O III] nebular line at 500.684 nm, while the dashed ones represent a mirror version of their red wings about a heliocentric radial velocity of 25 km s^{-1}.

Lyot atop Pic du Midi, in an attempt to detect the photospheric magnetic field invoked by Stahl et al. (1996) and Babel & Montmerle (1997b) to explain the periodic variability observed for θ^1 Ori C at X-ray, UV and optical wavelengths. These observations have also allowed us to detect an unexpectedly large and time variable level of continuum circular polarisation in the spectrum of θ^1 Ori C.

5.1. Magnetic field

We employed two different methods in order to determine an upper limit for the polar strength of the centred dipole magnetic field structure of Stahl et al. (1996). The conventional technique for estimating disc-averaged longitudinal fields yields non-detections with a 1σ error bar of about 250 G, implying that the polar field strength is lower than 1.6 to 2.0 kG (with a confidence level of 87%), depending on the exact orientation of the magnetic and rotation axes with respect to the line of sight. The more sophisticated method based on spectrum synthesis is usually more sensitive than the previous one, in particular to bipolar field structures that can potentially generate very large Zeeman signatures but are associated with very small values of the disc-averaged longitudinal field (e.g. Donati et al. 1997). For θ^1 Ori C however, the second method (yielding an upper limit on the polar field strength of 2.0 to 2.6 kG depending on the exact magnetic field geometry) finally turns out to be *less* sensitive than the first one, essentially because the intrinsic profile of θ^1 Ori C is much wider than the rotational profile and thus smoothes out all potential bipolar Zeeman signatures in the line profile (around phase 0.1 in our particular case).

We can therefore claim (with 87% confidence) that the polar strength of a centred dipole field in the photosphere of θ^1 Ori C is less than 1.6 to 2.0 kG (depending on the exact magnetic field geometry). This upper limit remains about 5 times larger than values derived from the MCWS model (Babel & Montmerle 1997b) and does therefore not provide very strong constraints on potential theoretical models for the variability of θ^1 Ori C. We should however be able to improve the situation in the very near future; using the Anglo-Australian Telescope and UCL échelle spectrograph fibre-fed from our visitor Cassegrain polarimeter (e.g. Donati et al. 1997), we estimate that we can obtain longitudinal field measurements with 1σ error bars of about 40 G within about 2 hr of observing thanks to both higher telescope photon collecting power ($4\times$) and better spectrograph throughput ($3\times$). The corresponding upper limit on the polar field strength should then be of the order of 250 to 300 G, just below the values inferred from the MCWS model.

5.2. Continuum polarisation

Strong levels of continuum circular polarisation (as much as 3.8% on 1997 Feb. 20) are detected in the spectrum of θ^1 Ori C, and further confirmed by the observation of depolarisation structures associated with all nebular emission lines. The shape and intensity of these depolarisation structures indicate that the production of continuum circular polarisation is confined to the immediate circumstellar environment. The continuum polarisation is variable on a day-to-day basis, possibly due to rotational modulation. The additional spectropolarimetric observations of θ^1 Ori C we obtained in 1998 (at rotational phases very close to those at which continuum polarisation was first detected) show no significant continuum polarisation nor depolarisation structures in nebular lines, indicating that this polarisation is also time variable on a long-term basis and probably related to a transient event.

Continuum circular polarisation is a fairly exotic astrophysical phenomenon. It can be produced at the few-percent level in some white dwarfs and neutron stars by the presence of multi-MG magnetic fields in their atmospheres (Angel et al. 1981). However, the flux ratio of a degenerate companion to θ^1 Ori C

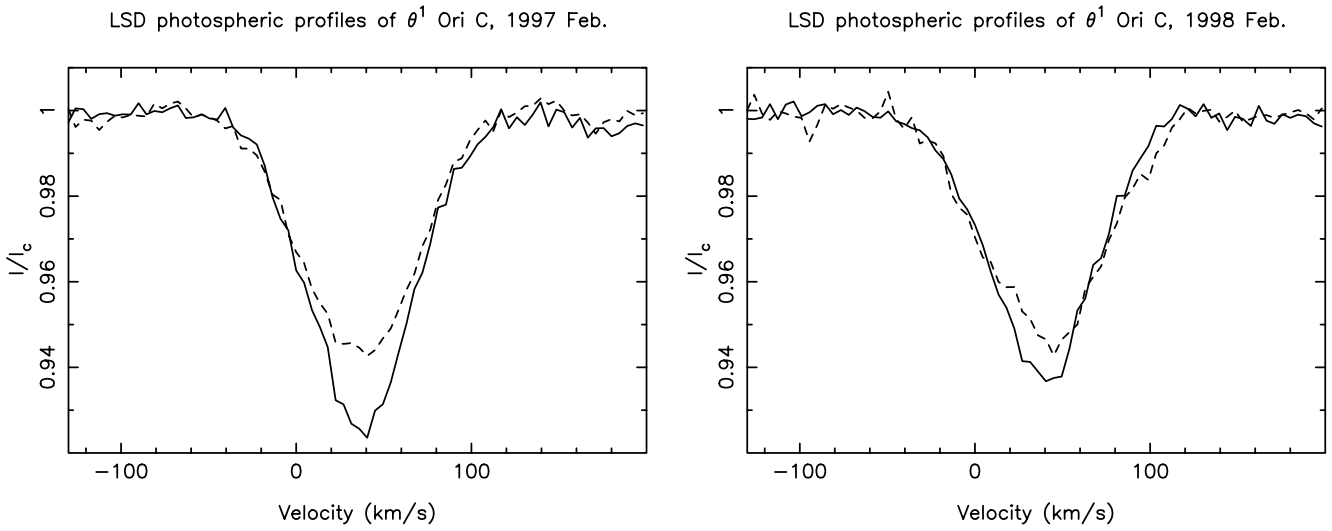

Fig. 4. LSD profiles of photospheric spectral lines of θ^1 Ori C in 1997 Feb. (*left panel*) and 1998 Feb. (*right panel*), closest to rotational phase 0.0 (full line) and phase 0.5 (dotted line). The exact rotational phases are 0.087 and 0.409 for 1997, and 0.136 and 0.428 for 1998 (see Table 1).

should be less than about 10^{-6} at visible wavelengths, even for the brightest white dwarfs (i.e. with an absolute visual magnitude of $M_{\rm V} \simeq 10$ compared to $M_{\rm V} = -4.5$ for θ^1 Ori C, Howarth & Prinja 1989). Any contribution to the continuum polarisation from a strongly magnetic degenerate companion is thus clearly negligible.

A second possibility is that birefringence in the interstellar medium converts linearly polarised light produced near the star into the observed circular polarisation. Although such a process is relatively common (Kemp & Wolstencroft 1972; Martin 1974), we do not expect it to be efficient enough in the particular direction of Orion (towards which interstellar polarisation does not exceed 1%, Leroy & Leborgne 1987) to account for the 3.8% of continuum circular polarisation that we detect.

A third source of continuum polarisation is scattering by electrons, atoms, molecules or other kinds of small particles (such as dust grains). In the particular case of spherical grains, single scattering produces only linear polarisation while circular polarisation can be generated through scattering of linearly polarised light and therefore multiple scattering processes (e.g. Ménard et al. 1988). Single scattering on more exotic non-spherical grains can even produce circular polarisation directly (Schmidt 1973, Bailey et al. 1998). Continuum circular polarisation has indeed been detected from some T Tauri stars, at a level of a few% (Chrysostomou et al. 1997). However, such processes usually require the star to be obscured by a highly anisotropic circumstellar environment, such as a circumstellar disc for instance.

It is therefore very tempting to invoke the circumstellar disc around θ^1 Ori C proposed by Stahl et al. (1996) and predicted by Babel & Montmerle (1997b) as a possible cause for the observed continuum circular polarisation. As suggested by Babel & Montmerle (1997b), this disc is probably responsible for the excess absorption observed in photospheric lines around rotational phase 0.0 (Stahl et al. 1996), i.e. when the disc is seen almost edge-on and comes in front of the visible stellar hemisphere. We may thus very well imagine that this disc is also responsible for scattering, and thus polarising, some of the stellar light. In particular, the fact that the highest rate of continuum polarisation is observed when the disc is seen edge on (close to phase 0.0) argues in favour of this interpretation. This scenario would however require that, around phase 0.0, as much as 3.8% of the stellar light is scattered by the disc towards the observer in the visible continuum (if the scattered light from the disc were 100% circularly polarised), and probably significantly more (since the scattered light is very likely only partially circularly polarised).

In this context, one would then expect to observe high rates of *linear* continuum polarisation (higher than 3.8% if we assume the scattering particles to be spherical for instance), in contradiction with published photopolarimetric observations of θ^1 Ori C reporting a rather low (although variable) level of continuum *linear* polarisation (of the order of 0.4%, Leroy & Leborgne 1987). In addition to this, we would expect to see weak photometric eclipses in visible light when the optically thin circumstellar disc predicted by Babel & Montmerle (1997b) comes in front of the visible stellar hemisphere (i.e. at phase 0.0) and scatters some of the stellar photons away from the line of sight. Although the exact eclipse contrast depends strongly on the physical details of the scattering processes (and in particular on the scattering phase functions), we can probably estimate that the number of photons scattered away from the line of sight is at least equal to the number of photons scattered towards the observer (i.e. larger than 3.8% of the stellar light), in contradiction with the observations of van Genderen et al. (1989) indicating that the star is not variable by more than 0.01 mag.

All observations may perhaps be reconciled if we keep in mind that the continuum polarisation we detected is *intrinsically* variable (in addition to the observed day-to-day variations presumably attributable to rotational modulation). We could imag-

ine for instance that during our 1997 Feb. observations, the circumstellar cooling disc (or at least some parts of it), while remaining optically thin, became temporarily denser than usual (by typically an order of magnitude) as a result of instabilities (Babel & Montmerle 1997a; Babel 1998), thereby increasing the amount of scattered light and continuum polarisation for a short time, and that the situation was back to normal in our 1998 Feb. run. If this scenario is correct, we would then expect at the same time to detect a larger *excess absorption* in photospheric spectral lines whenever the edge-on disc gets denser. As one can see from Fig. 4, the excess absorption of photospheric lines at phase 0.0 (relative to phase 0.5), while clearly detected at both epochs, is indeed significantly stronger in 1997 Feb. (Fig. 4, left panel) than one year later (Fig. 4, right panel). At the same time, we observe that, for *both* runs, equivalent widths of optical emission lines (and in particular Hα) are in good agreement with measurements of Stahl et al. (1996). It would imply that the density enhancement we invoke to explain qualitatively our continuum polarisation measurements, if real, is mainly confined to the cooler layers of the disc and does not extend to the hot layers above it and to the wind (where Hα is presumably formed, Babel & Montmerle 1997b).

Obviously, a more extensive investigation of this phenomenon is required through multicolour photometry, linear/circular spectropolarimetry and broadband photopolarimetry. However, the fact that similar events have never been reported yet in the literature (to our knowledge) probably indicates that they are not very frequent, implying at the same time that such a study will be difficult to undertake. A possibly fruitful direction of research could be to monitor the intrinsic *linear* continuum polarisation of θ^1 Ori C reported as variable by Leroy & Leborgne (1987) and search for a potential modulation with the rotational period of 15.426 d of Stahl (1998). If successful, this experiment may demonstrate that a circumstellar disc is indeed present around θ^1 Ori C, as proposed by Stahl et al. (1996) and predicted by Babel & Montmerle (1997b). It should help us as well to constrain its geometry and mean density, and thus to check whether the scenario we propose above is realistic.

Acknowledgements. We are very grateful to J. Oliveira for obtaining one of the MuSiCoS observations presented in this paper. Our thanks to J. Babel (as the referee), I.D. Howarth, J.D. Landstreet, J.-L. Leroy, F. Ménard, R. Oudmaijer and O. Stahl for advice related to this work and/or comments on earlier versions of this manuscript. GAW acknowledges support from the Natural Sciences and Engineering Research Council of Canada in the form of a Postgraduate Scholarship.

References

Angel J.R.P., Borra E.F., Landstreet J.D., 1981, ApJS 45, 457
Babel J., 1992, A&A 258, 449
Babel J., 1998, In: Wolf B., Fullerton A., Stahl O. (eds.) Variable and non-spherical stellar winds in luminous hot stars. IAU Coll. 169, Springer, Berlin, (in press)
Babel J., Montmerle T., 1997a, A&A 323, 121
Babel J., Montmerle T., 1997b, ApJ 485, L29
Bailey J., Chrysostomou A., Hough J.H., et al., 1998, Sci 281, 672
Baudrand J., Böhm T., 1992, A&A 259, 711
Castañeda H.O., 1988, ApJS 67, 93
Catala C., Foing B.H., Baudrand J., et al., 1993, A&A 275, 245
Chrysostomou A., Ménard F., Gledhill T.M., et al., 1997, MNRAS 285, 750
Donati J.-F., Catala C., Wade G.A., et al., 1998, A&AS (in press)
Donati J.-F., Semel M., Carter B., Rees D.E., Cameron A.C., 1997, MNRAS 291, 658
Gagné M., Caillaut J.-P., Stauffer J.R., Linsky J.L., 1997, ApJ 478, L87
Howarth I.D., Prinja R.K., 1989, ApJS 69, 527
Howarth I.D., Siebert K.W., Hussain G.A.J., Prinja R.K., 1997, MNRAS 284, 265
Kemp J.C., Wolstencroft R.D., 1972, ApJ 176, L115
Leroy J.-L., Leborgne J.-F., 1987, A&A 186, 322
Martin P.G., 1974, ApJ 187, 461
Mathys G., 1991, A&AS 89, 121
Mathys G., Manfroid J., 1985, A&AS 60, 17
Ménard F., Bastien P., Robert C., 1988, ApJ 335, 290
Preston G.W., 1967, ApJ 150, 547
Semel M., Donati J.-F., Rees D.E., 1993, A&A 278, 231
Schmidt T., 1973, In: Greenberg J.M., van de Hulst H.C. (eds.) Interstellar dust and related topics. IAU Symp. 52, Dordrecht, Boston, p. 131
Shore S.N., Brown D.N., 1990, ApJ 365, 665
Stahl O., 1998, In: Kaper L., Fullerton A. (eds.), Proc. of the ESO workshop on "Cyclical variability in stellar winds". Springer, Berlin, p. 246
Stahl O., Kaufer A., Rivinius T., et al., 1996, A&A 312, 539
Stahl O., Wolf B., Gäng T., et al., 1993, A&A 274, L29
van Genderen A.M., Bovenschen H., Engelsman E.C., et al., 1989, A&AS 79, 263
Wade G.A., Bohlender D.A., Brown D.N., et al., 1997a, A&A 320, 172
Wade G.A., Donati J.-F., Landstreet J.D., 1998a, MNRAS (submitted)
Wade G.A., Elkin V.G., Landstreet J.D., Romanyuk I.I., 1997b, MNRAS 292, 748
Wade G.A., Landstreet J.D., Donati J.-F., 1998b, A&A (submitted)
Wade R.A., Rucinski S.M., 1985, A&AS 60, 471
Walborn N.P., Nichols J.S., 1994, ApJ 425, L29